

UC Irvine

UC Irvine Previously Published Works

Title

DNA methylation patterns associated with konzo in Sub-Saharan Africa

Permalink

<https://escholarship.org/uc/item/60r4z7sw>

Journal

Clinical Epigenetics, 14(1)

ISSN

1868-7075

Authors

Kocher, Kristen

Bhattacharya, Surajit

Bramble, Matthew S

et al.

Publication Date

2022-12-01

DOI

10.1186/s13148-022-01372-x

Peer reviewed

BRIEF REPORT

Open Access



DNA methylation patterns associated with konzo in Sub-Saharan Africa

Kristen Kocher^{1,2}, Surajit Bhattacharya², Matthew S. Bramble^{1,2}, Daniel Okitundu-Luwa³, Dieudonne Mumba Ngoyi⁴, Desire Tshala-Katumbay^{3,4,5†} and Eric Vilain^{1,6*†}

Abstract

Konzo, a disease characterized by sudden, irreversible spastic paraparesis, affecting up to 10% of the population in some regions of Sub-Saharan Africa during outbreaks, is strongly associated with dietary exposure to cyanogenic bitter cassava. The molecular mechanisms underlying the development of konzo remain largely unknown. Here, through an analysis of 16 individuals with konzo and matched healthy controls from the same outbreak zones, we identified 117 differentially methylated loci involved in numerous biological processes that may identify cyanogenic-sensitive regions of the genome, providing the first study of epigenomic alterations associated with a clinical phenotype of konzo.

Keywords: Konzo, Epigenetics, DNA methylation, Cassava, Cyanide, Sub-Saharan Africa

Introduction

The World Health Organization (WHO) classifies konzo as a neurological disease characterized by sudden onset of spastic paraparesis in a formerly healthy individual and strongly correlated with the monotonous consumption of insufficiently processed bitter cassava (*Manihot esculenta Crantz*) and malnutrition, specifically a diet deficient in sulfur amino acids [1–4]. Cassava is a fibrous tuber and the predominant food source for many regions throughout Sub-Saharan Africa, including Angola, Cameroon, Central African Republic, Democratic Republic of the Congo (DRC), Mozambique, United Republic of Tanzania, and Zambia, which are the only countries in the world where konzo is endemic [1, 3, 4]. In addition to konzo, consumption of cyanogenic cassava has also been associated with other complex

neurodegenerative syndromes in Sub-Saharan Africa, including tropical ataxic neuropathy (TAN) and motor neuron-cerebellar-Parkinson-dementia syndrome [1, 5, 6]. Konzo is predominantly linked to rural regions in the seven aforementioned countries in Sub-Saharan Africa that lack healthcare infrastructure and resources [1, 3, 4]. The mean annual incidence rate of konzo diagnosis is 0.9 per 100,000 [1]. Studies have determined that cyanide exposure from cassava is associated with a loss of approximately 2 disability adjusted life years and an overall case-fatality ratio of about 21%, making konzo among the most prevalent of any disease associated with chemical exposure through the food supply [1].

Konzo onset typically occurs in a formerly healthy individual, beginning with bilateral spastic movements of the lower limbs that affect gait and progressing to exaggerated knee and ankle spasms, and occasionally full lower limb paralysis [2, 5, 7]. The disease is non-progressive and irreversible, without any apparent pathology of the spinal cord [2, 7]. Konzo can present in a spectrum of severities and occur with comorbidities, such as cognitive impairment [6, 7]. Epidemiological surveys have highlighted that children and women of child-bearing age

[†]Desire Tshala-Katumbay and Eric Vilain contributed equally to this manuscript.

*Correspondence: evilain@hs.uci.edu

⁶Institute for Clinical and Translational Science, University of California, Irvine, Irvine, CA 92697, USA
Full list of author information is available at the end of the article



© The Author(s) 2022. **Open Access** This article is licensed under a Creative Commons Attribution 4.0 International License, which permits use, sharing, adaptation, distribution and reproduction in any medium or format, as long as you give appropriate credit to the original author(s) and the source, provide a link to the Creative Commons licence, and indicate if changes were made. The images or other third party material in this article are included in the article's Creative Commons licence, unless indicated otherwise in a credit line to the material. If material is not included in the article's Creative Commons licence and your intended use is not permitted by statutory regulation or exceeds the permitted use, you will need to obtain permission directly from the copyright holder. To view a copy of this licence, visit <http://creativecommons.org/licenses/by/4.0/>. The Creative Commons Public Domain Dedication waiver (<http://creativecommons.org/publicdomain/zero/1.0/>) applies to the data made available in this article, unless otherwise stated in a credit line to the data.

appear to be more vulnerable to developing konzo, and familial clusters of disease occur for reasons that have yet to be fully elucidated [8].

Uncovering the molecular underpinnings of konzo etiology and its comorbidities are of considerable interest, as cassava is a dietary staple for over 800 million people due to its drought tolerance [1]. All cultivars of cassava have an innately high concentration of the cyanogenic glucosides, predominantly linamarin, which assist in defending the tuber from animals and insects [1]. Proper processing of cassava makes it safe to consume and is crucial to reducing the concentration of linamarin and downstream cyanide exposure [1, 6]. During times of drought, famine, and war, when resources and time are scarce, proper processing techniques diminish and epidemics of konzo become rampant [1, 6].

As konzo can affect up to 10% of the population in regions throughout Sub-Saharan Africa that subsist on a homogenous diet of cassava, it is of critical importance to elucidate the pathophysiologic factors that contribute to disease susceptibility and onset [5]. As epigenetics are known to be heavily influenced by the environment, age, and diet, this study focuses on detecting the underlying epigenomic signatures in individuals in areas of konzo-outbreaks compared to age-matched and sex-matched, unaffected controls from the same outbreak zones in the DRC. DNA methylation has been shown to be a genomic marker of exposure to certain chemicals and thus can be used as a diagnostic signature for poorly understood, environment-induced diseases [9]. By highlighting loci within the genome that are differentially methylated we will be able to better understand the individual susceptibility risks of konzo. This is the first study focused on understanding the underlying epigenomic signatures, or biomarkers, associated with konzo. Future studies should aim to focus on functional validation of the apparent molecular differences highlighted in this study, including extent of dietary exposure, toxicity, and adverse outcome pathways, and explore the complex epigenetic and transcriptional landscape associated with sub-lethal cyanide exposure and the clinical konzo phenotype.

Methods

Patient samples

Samples from the konzo outbreak regions of Kahemba, southern Bandundu Province, DRC, were obtained in October to November 2011; samples from the konzo outbreak region in of zone de sane de Mwana, South Kivu Province, were collected in November 2012. From a previously established konzo WHO surveillance list of outbreaks in Kahemba and South Kivu, subjects were identified and used for this study [10]. The institutional review board at Oregon Health and Sciences University

and the Democratic Republic of the Congo Ministry of Health provided study approval. Enrolled children were consented by caregivers orally in the local language with signature or thumb print for those not literate. Individuals were phenotypically diagnosed using neurological exam performed by neurologists to confirm konzo diagnosis using the 1996 WHO criteria. For konzo-affected individuals, konzo severity was described as “mildly abnormal (periodic or mild hyperreflexia and exaggerated clonus or reflexive delay)”. Patient demographic data can be found in Additional file 1: Table S1.

Whole blood was collected in EDTA tubes from healthy and konzo-affected individuals by local medical staff at two sites in DRC (Kahemba and South Kivu) and separated into serum, buffy coat, and plasma at the collection site and then stored in liquid nitrogen until DNA processing. DNA was extracted from buffy coat and stored at -80°C in the Tshala-Katumbay lab (University of Kinshasa, DRC). Samples were transported for long-term storage to the Tshala-Katumbay lab at Oregon Health & Science University (Portland, OR, USA), until they were used for DNA methylation experiments ($n=32$) and transferred to Children’s National Research Institute (Washington DC, USA).

Genome-wide DNA methylation array

DNA was quantified using the Qubit dsDNA Broad Range Assay kit and Qubit 4 fluorometer (Thermo Fisher). 300 ng of extracted DNA from each sample was bisulfite converted using the EZ DNA Methylation-Lightning kit (Zymo). Samples were whole-genome amplified, enzymatically fragmented, and hybridized to BeadChip array using the Infinium MethylationEPIC BeadChip kit according to the manufacturer’s protocol (Illumina). Hybridized methylation arrays were scanned using the iScan system (Illumina) at Georgetown University’s Genomics & Epigenomics Shared Resource Core in Washington, DC. The Gene Expression Omnibus accession number is GSE18011.

Methylation array analysis

Raw intensity values (idat files) were generated from each EPIC BeadChip row using the iScan system. All statistical analysis was done using R (version 4.0.1) and Bioconductor packages. Intensity values were converted to beta (β) and m values using the Bioconductor *minfi* package. β values ($\beta = M/(M+U+100)$, where M is methylated intensity and U is unmethylated intensity for the same position) are used for visualization and m value ($M = \log_2(M/U)$) for statistical analyses (difference in average konzo β values = 0.29; difference in average control β values = 0.35; Additional file 1: Table S2). Quality filtration parameters, used to filter out low quality

probes, were probes that are represented by less than 3 beads for greater than 5% of the samples (49,632 probes), probes having quality p value less than 0.05 (15,032 probes), probes having SNP (9956 probes), and probes mapping to multiple sites in the genome (“cross-reactive probes”; 41,482 probes). Probes filtered for quality p values and SNP probes were determined by *detectionP* and *dropLociWithSnps* functions of the *minfi* package, cross-reactive probes by *dropXreactiveLoci* function of the *maxprobes* package and bead related filtration by *beadcount* function of the *wateRmelon* package [9]. The probe intensity was normalized by Subset-quantile Within Array Normalization (SWAN). A total of 795,169 quality filtered normalized probes were used for subsequent differential methylation analysis using *limma* package in R. Differential DNA methylation analysis was performed using a statistical threshold cutoff FDR $p \leq 0.05$ and log₂ fold-change cutoff of < -1 or > 1 (Additional file 1: Table S4). Quality visualization was done using *champ.QC* function of *ChAMP* package in R, and PCA plots were done using base R package. Tool information and references can be found in Additional file 1: Table S3. Data quality plots can be found in Additional file 2: Fig. S1. Sex-prediction analysis did correctly predict the sexes of all but one sample, K16. Additionally, we performed immune-cell variation analysis using *FlowSorted.Blood.EPIC* package to determine any potential involvement of immune cell fractions in this analysis by calculating the means per cell type and cohort (Fig. 1C, Additional file 1: Table S5 and S6) and sex-prediction analysis through *minfi*. There were no immune-cell fraction differences between konzo cases and controls and the resultant gene list contained 76% of the resultant genes from the analysis prior to performing immune-cell fraction analysis.

Gene ontology enrichment analysis

Functional annotation was done using Enrichr (<https://maayanlab.cloud/Enrichr/>) on all differentially methylated probes that appeared in promoter region (defined as either located in the transcription start site (TSS) or 5' UTR) choosing only gene ontology terms enriched for “Biological Processes” with a statistical significance of $p \leq 0.05$. Duplicated or redundant gene ontology terms were reduced through the REVIGO interface using standard parameters and visualized using GOplot (details in Additional file 1: Table S7).

Validation of array-based DNA methylation signatures

A targeted next-generation bisulfite sequencing panel was chosen based on 33 probes (Illumina IDs) that were noted to be differentially methylated between cases and controls from our array analysis and used to validate our findings (EpiGenDx). For validation, we chose 8 cases

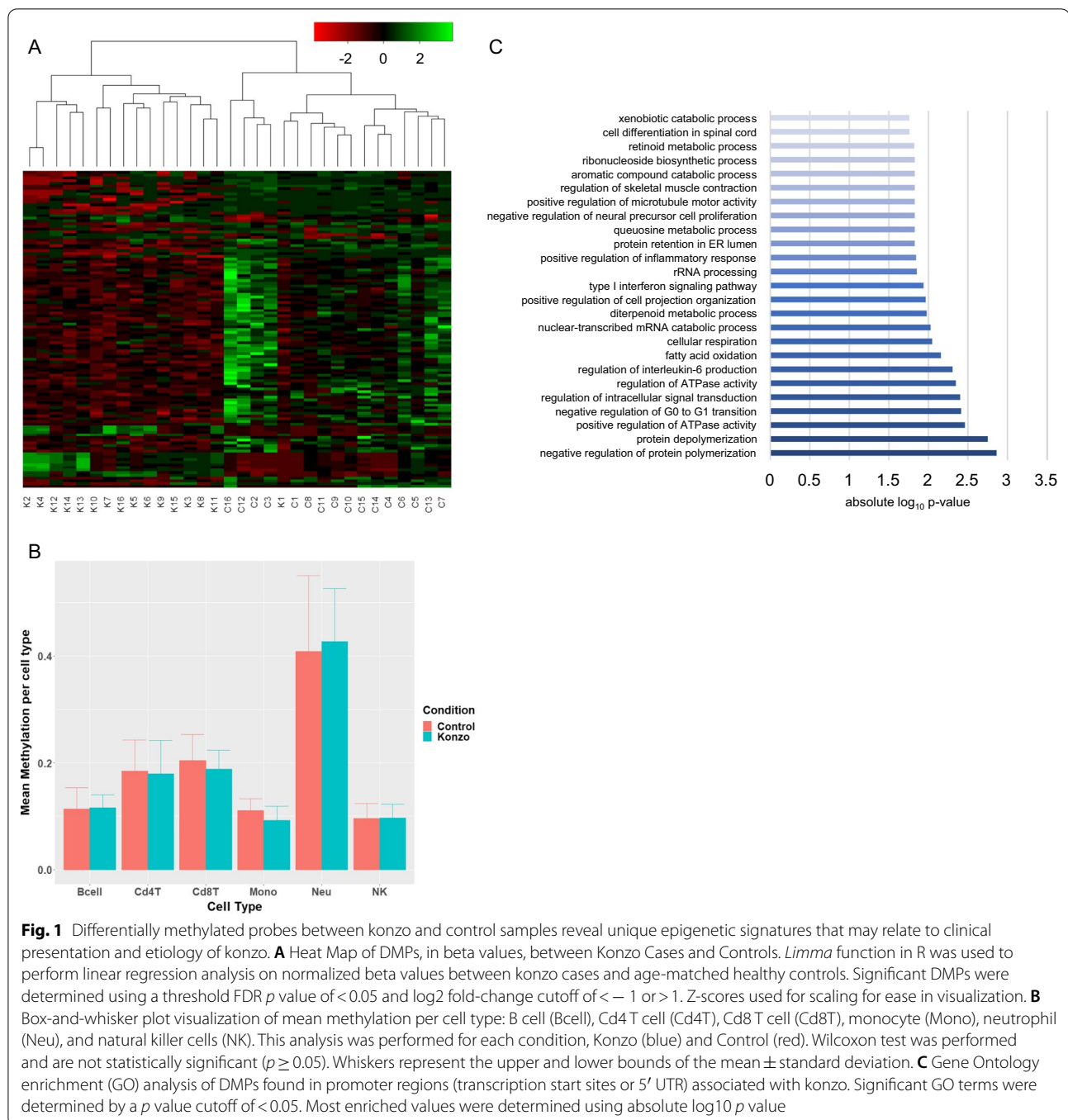
and 8 control samples from our original array analysis and 33 previously identified probe locations of differential methylation (Additional file 1: Table S8). We shipped eluted DNA to EpiGenDx, where they performed bisulfite modification, multiplex PCR, library preparation, and sequencing (Ion Torrent S5). FASTQ files were aligned with Bismark Bisulfite Read Mapper program (v0.12.2) and Bowtie2 (v2.2.3), and Bismark was used to calculate methylation levels. T test was performed to identify difference between the 2 conditions, with significance thresholds.

Results and discussion

Comparative analysis of normalized intensities derived from interrogation of over 850,000 methylation probe sites between konzo cases and age- and sex-matched healthy controls suggests that there are 117 differentially methylated probes (DMPs) significantly associated with konzo-affected individuals (Fig. 1A). Of the 117 total sites of differential methylation, 99 DMPs were hypomethylated, while 18 sites were hypermethylated compared to controls (Additional file 1: Table S4). The EPIC array data were validated using next-generation targeted bisulfite sequencing, which confirmed our findings at 33 of the most differentially methylated sites (Additional file 1: Table S3). Unsupervised hierarchical clustering of DMP intensities revealed that samples cluster strongly by cohort, except for one sample (K1), which appears to cluster more with the control cohort than konzo (Fig. 1A). Without other clinical information, it is not possible to determine if this sample is clustering differently due to other phenotypic associations (i.e., disease onset or severity) or a true outlier of the study. We did however rule out the influence of immune-cell-type contributions, which were not observed to be significantly different in our analysis (Fig. 1B).

Since there are apparent sex-specific differences in the manifestation and presentation of konzo, where females of child-bearing age appear to be more vulnerable than males (although this may be attributed to social differences), we interrogated konzo males versus konzo females and did not identify significantly differentially methylated loci attributed to sex (data not shown) [7]. However, the analyzed cohort is small and may not have had enough statistical power to uncover sex-specific differences in DNA methylation associated with disease [7].

Of the 117 DMPs between konzo and controls, there were 2 genes with multiple differentially methylated probes that were significantly differentially methylated in the konzo cohort, *ZNF718* and *AKAP12* (Additional file 1: Table S4). All sites associated with the genes *ZNF718* and *AKAP12* were significantly hypermethylated (FDR p value ≤ 0.05 and log₂ fold-change in DNA



methylation intensity ≤ 1) in konzo cases, compared to controls (Additional file 1: Table S4). 46 of these sites associated with genes were identified in the promoter region (TSS or 5' UTR). These 46 sites were analyzed for gene ontology (GO) enrichment at a statistical threshold of $p \leq 0.05$ and we were able to ascertain that the konzo cohort was enriched for biological processes relevant to konzo etiology and potentially relevant pathways

(Fig. 1C, Additional file 1: Table S7). For example, among the top enriched terms, we noted *regulation of skeletal muscle contraction* (GO: 0014819), which may be directly relevant to the spastic movements and paraparesis that are characteristically associated with the konzo phenotype (Fig. 1C) [2]. Additionally, using the Online Mendelian Inheritance of Man database, we identified that the associated gene for this GO term, *KCNJ2*, has been

implicated in other disorders of periodic paralysis, such as Andersen Syndrome, and thus may be directly relevant to konzo disease presentation [11].

Of additional interest, we noted significant enrichment for the biological process *queuosine metabolic process* (GO: 0046116). Queuosine is a modified nucleoside present in certain mammalian tRNAs and its abundance has been linked to the presence of micronutrients derived from the gut microbiome and directly links to transcriptional regulation [12, 13]. As konzo onset is linked not only to dietary exposure to cyanogenic glucosides, but also to SAA deficiency, an adjunct role of the gut microbiome could also play into the disease phenotype and be linked to changes in DNA methylation, transcription, and metabolic processes. The literature suggests that DNA methylation is strongly influenced by the environment, so changes in diet that are known to be associated with disruptions in molecular processes and the gut microbiome, like queuosine metabolism, may be of interest for elucidating the complex mechanisms associated with konzo disease onset and progression.

Overall, while enrichment of these biological processes may suggest a role for modifications to DNA methylation in disease phenotype, these 117 sites of differential methylation may serve as biomarkers for monitoring populations at-risk for konzo. Functional validation is critical to further explore these findings and understand the impact of these differentially methylated sites in the context of dietary cyanogenic glucoside exposure and konzo presentation, as well as determine if there are specific epigenetic markers associated with susceptibility or risk to developing a clinical phenotype, as konzo does not present in all who are exposed to the same, homogenous diet of cyanogenic cassava.

A limitation of this study is the small sample size ($n=32$) that was used. While we were able to determine statistically significant DNA methylation differences between our cohorts, future studies should look to expand on the size of the cohort used, increase the age range, and include numerous disease severity levels, and ensure that a sufficient sample size is used for a well-powered study. Additionally, by correlating the level of in vivo cyanogenic glucoside metabolites in serum or urine at the time of collection could provide invaluable information regarding the level exposure of each individual to cyanogenic cassava through the diet and further be associated with the DNA methylation changes present. As previously mentioned, children are also at high-risk groups for developing konzo. In this cohort, the median age of recruited konzo and healthy control individuals was approximately 13 years old. As such, we are unable to draw conclusions regarding the DNA methylation patterns associated with pediatric versus adolescent ages

groups. Future research should aim to observe longitudinal progression of this disease and consider timing of onset and severity of these age groups, which may elucidate the molecular underpinnings of the sudden and irreversible phenotype associated with konzo.

This study has provided the first analysis of epigenetic changes associated with clinical diagnosis of konzo. Future experiments should focus on further identifying biomarkers of low-dose dietary cyanide exposure and identifying factors of konzo disease susceptibility and pathobiology through other molecular approaches.

Abbreviations

DRC: The Democratic Republic of the Congo; TAN: Tropical ataxic neuropathy; DMP: Differentially methylated probe; SWAN: Subset-quantile within array normalization; GO: Gene ontology.

Supplementary Information

The online version contains supplementary material available at <https://doi.org/10.1186/s13148-022-01372-x>.

Additional file 1: Table S1. Sample collection information. Sample IDs were relabeled with "Analysis ID" for improved readability on figures. Cohort specific information, location of sample collection, and age are also provided (average age = 13 years old). **Table S2.** Beta values of all konzo case and control samples. Beta values for individual konzo samples are labeled columns K1–K16; beta values for individual control samples are labeled C1–C16. Averages for both groups are labeled Average_Konzo_Bvalue and Average_Contrl_Bvalue. Mean for each group is labeled Average_Konzo_Bvalue_Total and Average_Contrl_Bvalue_Total. **Table S3.** DNA Methylation analysis tools, functions and references. **Table S4.** Output significantly differentially methylated probes from bioinformatic analysis. Threshold for significance: FDR p value < 0.05, log₂ fold-change of less than or equal to -1 or greater than or equal to 1. Column headers include the Illumina ID (IllumID), Chromosome Number (Chromosome) and location (Coordinate_start or Coordinate_end), positive or negative strand (Strand), gene name (Name), location of probe to CpG (Group), log₂ fold-change value (logFC), and FDR adjusted p value (adj.PVal). **Table S5.** Output significantly differentially methylated probes from bioinformatic analysis with immune cell fraction analysis. Threshold for significance: FDR p value < 0.05, log₂ fold-change of less than or equal to -1 or greater than or equal to 1. Column headers include the Illumina ID (IllumID), Chromosome Number (Chromosome) and Location (Coordinate_start or Coordinate_end), positive or negative strand (Strand), gene name (Name), location of probe to CpG (Group), log₂ fold-change value (logFC), and FDR adjusted p value (adj.PVal). **Table S6.** Cell-type fraction means for Konzo cases and controls. Standard deviation (sd) was calculated for each mean. Column headers include: cell type (CellType), cohort specifics (Condition), mean (Mean), standard deviation (sd), and Upper (mean + sd) and Lower (mean-sd) bounds. **Table S7.** Output significantly enriched GO Terms. Threshold for significance: p value < 0.05. Column headers include the GO ID (ID), GO Term Description (GO Description), absolute log₁₀ p value (abs_log10_pval), log₁₀ p value (log10_pval), p value (pval), and genes associated with GO ID (genes). **Table S8.** Targeted methylation analysis results. ProbelID: Illumina probe IDs; Genes: Associated genes; Transcripts: Associated transcripts; Chromosome: chromosomal position; Region: Regions in the chromosome that get affected; %MethylationDifference: Difference in methylation percentage; logFC: Difference in log (base 2) fold change; p value: associated p value.

Additional file 2: Fig. S1. Principal component analysis (PCA) plots show similarity in signal intensity between konzo and control samples. **A** PCA plot for signal intensity of all control and konzo samples before normalization: Principal component analysis done on more than 850 K probes (866,087 probes), reveals a tighter overlap of intensities (principal

components) between Konzo samples (blue) compared to red (Control) samples. There is some overlap with between the controls and the Konzo sample, which might lead to the assumption that there is not a huge difference in the epigenetic patterns between konzo and control samples. **B** PCA plot for signal intensity of all control and konzo samples after filtration and SWAN normalization: Principal component analysis done on more than 795,169 probes, reveals similar pattern to before normalization, leading to the assumption that there is not much difference in epigenetic signature between the conditions.

Acknowledgements

We would like to thank the Congolese participants of this study for kindly donating specimens. We would also to acknowledge the passing of Jean-Pierre Banea Mayambu, a pioneer in the field of konzo, who will truly be missed.

Author contributions

KK contributed to quality control and bisulfite conversion of DNA samples, Infinium MethylationEPIC BeadChip array protocol and scanning of arrays, collection of raw data and bioinformatic analysis, and targeted bisulfite sequencing. SB contributed to bioinformatic analysis of data, GO enrichment analysis, and generation of figures and tables. MB contributed to experimental design and data analysis. DOL and DMN contributed to recruited, consented, collected participants for study in DRC, and revised manuscript. DTK contributed to design and ethics approval for study and supervised data analysis and interpretation. EV contributed to experimental design, supervised data analysis and interpretation. All authors contributed to the content of the manuscript. All authors read and approved the final manuscript.

Funding

We would also like to thank the funding sources for this project, with DTK being supported by NIH grant NIEHS/FIC R01ES019841, EV being supported by the A. James Clark Distinguished Professor of Molecular Genetics Endowment and MSB being supported by the Fogarty International Center of the National Institutes of Health (NIH) under Award Number D43TW009343 and the University of California Global Health Institute (UCGHI); the content is solely the responsibility of the authors and does not necessarily represent the official views of the NIH or UCGHI. MSB is supported by the Fogarty International Center of the National Institutes of Health (NIH) under award number 5K01TW011772-02.

Availability of data and materials

The datasets generated and analyzed during the current study are available in the GEO repository (GSE180119), <https://www.ncbi.nlm.nih.gov/geo/query/acc.cgi?acc=GSE180119>.

Declarations

Ethics approval and consent to participate

Informed consents were obtained verbally by investigators who are fluent in Lingala and/or Kikongo the local spoken languages. Ethical approval of research activities including informed consent was obtained from the Oregon Health & Science University (OSHU) IRB FWA00000161 and from the Ministry of Health of the Democratic Republic of the Congo (DRC).

Consent for publication

Not applicable.

Competing interests

The authors declare that they have no competing interests.

Author details

¹Department of Genomics and Precision Medicine, The George Washington University School of Medicine and Health Sciences, Washington, DC 20037, USA. ²Department of Genetic Medicine Research, Children's Research Institute, Children's National Hospital, Washington, DC 20010, USA. ³Department of Neurology, University of Kinshasa, Kinshasa, Democratic Republic of the Congo. ⁴National Institute of Biomedical Research, Kinshasa, Democratic Republic

of the Congo. ⁵Department of Neurology, School of Medicine, Oregon Health and Science University, Portland, OR 97239, USA. ⁶Institute for Clinical and Translational Science, University of California, Irvine, Irvine, CA 92697, USA.

Received: 15 April 2022 Accepted: 8 November 2022

Published online: 19 December 2022

References

- Gibb H, Devleeschauwer B, Bolger PM, Wu F, Ezendam J, Cliff J, et al. World Health Organization estimates of the global and regional disease burden of four foodborne chemical toxins, 2010: a data synthesis. *F1000Research* [Internet]. 2015;1–14. <http://f1000research.com/articles/4-1393/v1>.
- Tylleskär T, Howlett WP, Rwiza HT, Aquilonius SM, Ståhlberg E, Linden B, et al. Konzo: a distinct disease entity with selective upper motor neuron damage. *J Neurol Neurosurg Psychiatry*. 1993;56(6):638–43.
- Siddiqi OK, Kapina M, Kumar R, Ngomah Moraes A, Kabwe P, Mazaba ML, et al. Konzo outbreak in the Western Province of Zambia. *Neurology*. 2020;94(14):e1495–e1501.
- Baguma M, Nzabara F, Maheshe Balemba G, Malembaka EB, Migabo C, Mudumbi G, et al. Konzo risk factors, determinants and etiopathogenesis: what is new? A systematic review. *Neurotoxicology*. 2021;85:54–67.
- Tshala-Katumbay D, Mumba N, Okitundu L, Kazadi K, Banea M, Tylleskär T, et al. Cassava food toxins, Konzo disease, and neurodegeneration in sub-Saharan Africans. *Neurology*. 2013;10:949–51.
- Tshala-Katumbay DD, Ngombe NN, Okitundu D, David L, Westaway SK, Boivin MJ, et al. Cyanide and the human brain: perspectives from a model of food (cassava) poisoning. *Ann N Y Acad Sci*. 2016;1378(1):50–7.
- Boivin MJ, Okitundu D, Makila-Mabe B, Sombo MT, Mumba D, Sikorskii A, et al. Cognitive and motor performance in Congolese children with konzo during 4 years of follow-up: a longitudinal analysis. *Lancet Glob Heal* [Internet]. 2017;5(9):e936–47. [https://doi.org/10.1016/S2214-109X\(17\)30267-X](https://doi.org/10.1016/S2214-109X(17)30267-X).
- Diasolua Ngudi D, Banea-Mayambu JP, Lambein F, Kolsteren P. Konzo and dietary pattern in cassava-consuming populations of Popokabaka, Democratic Republic of Congo. *Food Chem Toxicol* [Internet]. 2011;49(3):613–9. <https://doi.org/10.1016/j.fct.2010.06.053>.
- Meehan RR, Thomson JP, Lentini A, Nestor CE, Pennings S. DNA methylation as a genomic marker of exposure to chemical and environmental agents. *Curr Opin Chem Biol* [Internet]. 2018;45:48–56. <https://doi.org/10.1016/j.cbpa.2018.02.006>.
- Boivin MJ, Okitundu D, Makila-Mabe Bumoko G, Sombo M-T, Mumba D, Tylleskär T, et al. Neuropsychological effects of Konzo: a neuromotor disease associated with poorly processed cassava. *Pediatrics* [Internet]. 2013;131(4):e1231–9. <https://doi.org/10.1542/peds.2012-3011>.
- Fialho D, Griggs RC, Matthews E. Periodic paralysis. *Handb Clin Neurol*. 2018;148:505–20.
- Tuorto F, Legrand C, Cirzi C, Federico G, Liebers R, Müller M, et al. Queuosine-modified tRNAs confer nutritional control of protein translation. *EMBO J*. 2018;37:e99777.
- Huber SM, Leonardi A, Dedon PC, Begley TJ. The versatile roles of the tRNA epitranscriptome during cellular responses to toxic exposures and environmental stress. *Toxics*. 2019;7:17.

Publisher's Note

Springer Nature remains neutral with regard to jurisdictional claims in published maps and institutional affiliations.